Behaviour of anisotropic rocks

Authors: M. Sc. Mohamed Ismael, M. Sc. Lifu Chang & Prof. Dr.-Ing. habil. Heinz Konietzky (Geotechnical Institute, TU Bergakademie Freiberg)

Editor: Prof. Dr.-Ing. habil. Heinz Konietzky Layout: Angela Griebsch, Gunther Lüttschwager
TU Bergakademie Freiberg, Institut für Geotechnik, Gustav-Zeuner-Straße 1, 09599 Freiberg • sekr_fm@ifgt.tu-freiberg.de

1 Introduction

Rock nature is widely different than soil or concrete, most of failure criterions which are addressed to CHILE material (Continuous, Homogeneous, Isotropic and Linear-elastic material) are not applicable for the rock material (Hudson & Harrison 1997), as rocks are totally different and more complicated than this definitions. Generally, rock material is mostly intersected by various layers and joints (Discontinuities) due to the geological features and tectonic movements. Through the extensive studying of the mechanics of rocks and their behaviour, it is found that most of rock materials are considered as anisotropic material. Analysing, modelling and simulating the anisotropy of rocks attracted different researchers since 1960s. In this chapter, we are providing a discussion about the reasons of taking into account the anisotropy of rocks and different ways of modelling this characteristics of rocks.

2 Features causing rock anisotropy

Rocks are defined as a mechanical bonding of the grains of one mineral (mono mineral rock) or more than one mineral (Poly-mineral rock), this mechanical bonding depends on the origin of the rock, whether it is igneous, metamorphic or sedimentary rock. During the formation of different types of rocks there are different processes taking place which are categorized into both primary and secondary structures. In following points we are going through the main geological features that cause the rock anisotropy.

2.1 Primary structures

Micro geological features are named also the primary structures which are found during the formation stage of different rocks. These features influence the rock anisotropy by: rock fabric anisotropy, texture, schistosity and fissility. They are mainly found in the microscopic scale and also are related to the grain size. In general, the anisotropic behaviour of the rocks mainly depending on the textures and fabric of the principal rock-forming minerals (the microscopic fabric) (Ullemeyer et al. 2006).

According to (Bagheripour et al. 2011), the anisotropic nature of rocks is found at:

- (1) Most foliated metamorphic rocks, such as schist, slates, gneisses and phyllites, contain a natural orientation in their flat/long minerals or a banding phenomenon which results in anisotropy in their mechanical properties. Figure 1 shows some features of texture anisotropy in a metamorphic slate unit such as: layering and intersecting of planar fabric.

- (2) Stratified sedimentary rocks like sandstone, shale or sandstone - shale alteration often display anisotropic behaviours due to presence of bedding planes. The major reason for the anisotropy in sedimentary rocks is related to the sedimentation processes of the different layers (strata) or different minerals with various grain sizes. In Fig. 2, there is a sample of bedding which is found in shale. Fissility is a special geological feature concerns the sedimentary rocks in which grains are deposited forming parallel set of planes and the rock unit fails by the slipping along these planes. However, the fissility of the laminated rocks is considered as a structure related mostly to the sedimentary rocks such as siltstone and it is metamorphosed into the foliation (Van Hise 1896).

- (3) Anisotropy can also be exhibited by igneous rocks having flow structures as may be observed in porous rhyolites due to weathering (Matsukura, Hashizume, and Oguchi 2002). Generally, igneous rocks have few possibility of fabric anisotropy. But in some cases, the anisotropy may be found due to layering when the lava flows and moves as highly viscous masses immediately before the consolidation (such as granite) (Walhlstrom 1973).

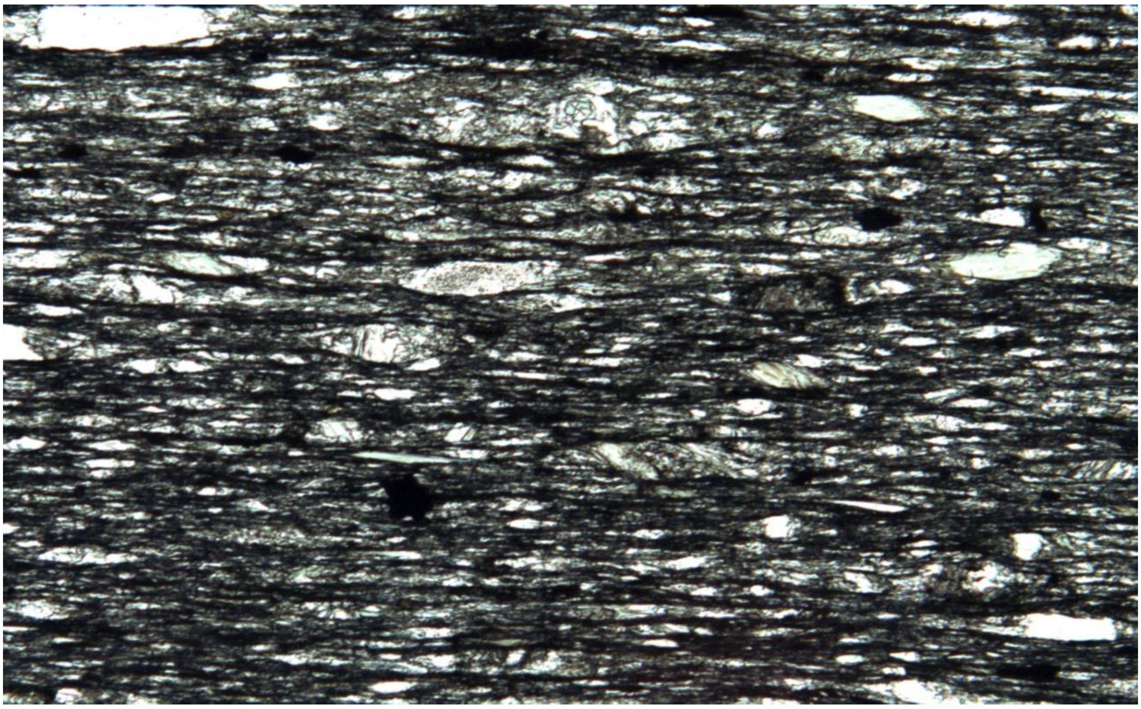

Fig. 1: Sample of slate- layering and intersecting of planar fabric.

Fig. 2: Sample of sedimentary: shale bedding.

2.2 Secondary structures

Secondary structures are known also as the macro-scale features of rocks which are defined by one word as "discontinuities". They are defined as: (i) cracks and fractures, (ii) bedding planes and (iii) shear planes and faults (Salager et al. 2013). Such features' influence is significant and associated with three distinct issues (Bobet et al. 2009):

(i) The scale: which effects the modelling of these planes implicitly or explicitly,
(ii) stress and/or displacement conducted: these planes significantly reduce the rock strength, and
(iii) relative motions of rock blocks: the discontinuity limits the elastic behaviour of the rock material.

The effect of a single plane of weakness on the strength anisotropy is introduced by (Jaeger, J. C. & Cook 1979).

Even (Hoek 1983) has developed a criterion to express the strength of the jointed rock mass, and it is concluded as:

(i) The rock strength of jointed rock depends completely on the degree of the interlocking of rock blocks,
(ii) Rocks with a single joint set behave highly anisotropic, and
(iii) The strength behaviour of rock masses having three, four or five intersecting joint sets are considered approximately homogenous and isotropic.

So how these geological features and anisotropy characteristic influence the rock parameters and behaviour, this is what we are discussing later.

2.3 Discontinuity frequency

Discontinuous frequency can be defined linearly or by the unit volume, whereas the frequency can be expressed as the number of the discontinuities by either unit length or unit volume (Priest 1993). The anisotropy of the discontinuity frequency comes from the variations of the discontinuity spacing in reference to the orientation of the scanline or the studied volume of the rock mass (Hudson & Harrison 1997). As in Fig. 3, the idea of the anisotropy due to the variation in the scan line for the same discontinuities is clear, the spacing between the discontinuities is a function of the orientation of the scanline (X ≠ Y).

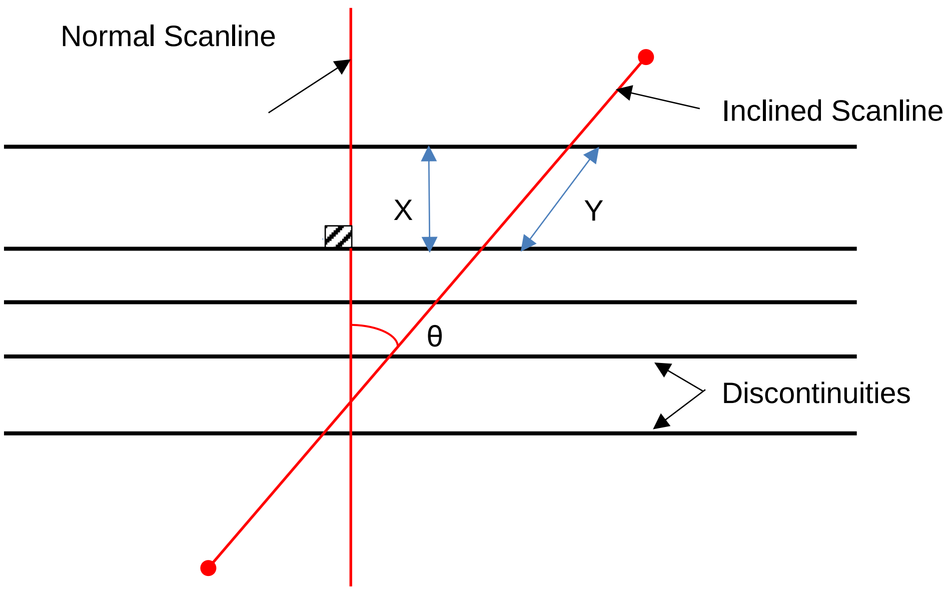

Fig. 3: Two different discontinuities frequencies due to the orientation of the scanlines

Thus, it is mandatory to rotate all the scanline to one fixed orientation to define the accurate frequency of discontinuities, which means to define all the discontinuities dip angles and dip directions. This method may be applicable if the discontinuities are represented as parallel sets but it will be more complicated for curved or more complex shapes of discontinuities. It is important to depend on the volumetric fracture density because it is independent of direction and it is considered as a static parameter (Singhal & Gupta 2010).

3 Observation and measurement of rock anisotropy

For the characterization of rock anisotropy most of all the following parameters are used:

3.1 Strength anisotropy

Anisotropy of rock strength means that the rock strength is a function of the angle between loading direction and orientation of the anisotropy planes. For simplicity and due to the fact that this constellation is often met in engineering practice and lab testing, let us consider uniaxial loading of a rock sample with one plane of weakness. In that case the minimum strength value will be found usually at β_{min} = 30° and 45° (β is the angle between loading direction and plane of weakness, see also chapter 5.3.3). The magnitude of the strength changes according to the orientation of the inherent planes of weakness. Saroglou and Tsiambaos (2008) have tested different types of metamorphic rock. Fig. 4 shows the obtained uniaxial compressive strength (UCS) values as function of orientation angle β . This diagram shows, that some rocks show pronounced anisotropy in strength, others not or only marginal.

Jaeger & Cook (1979) discussed the failure of the anisotropic rocks under confining pressure. Equation 1 describes the uniaxial compressive strength of a sample with weak plane, which is characterized by cohesion C_j and friction angle ϕ. Under the assumption that rock matrix has infinite strength, a result like shown in Fig. 5a is obtained.

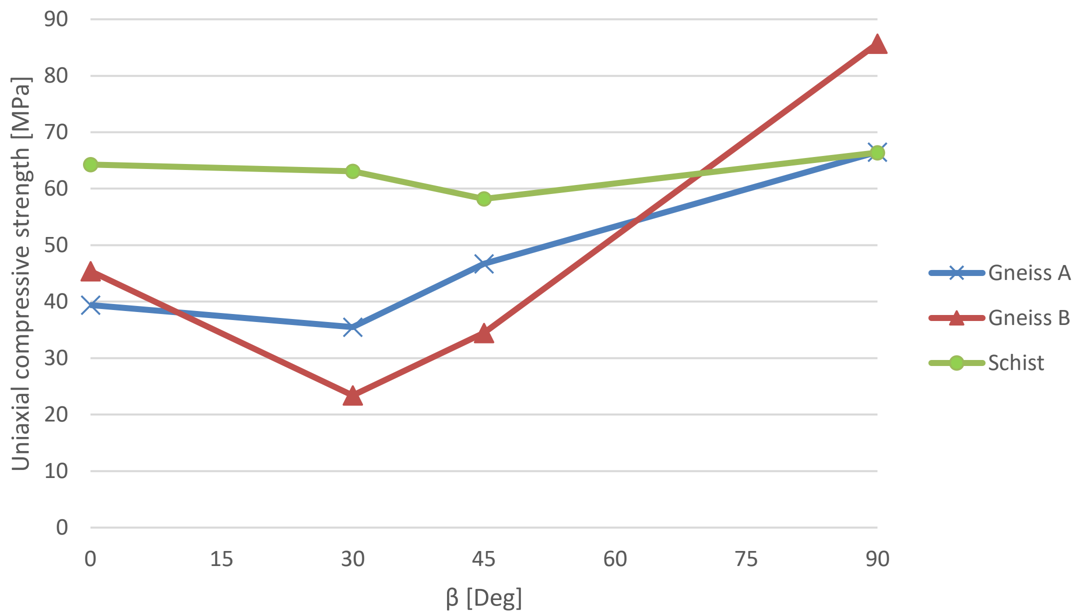

Fig. 4: Uniaxial compressive strength versus orientation angle β (modified after Saroglou and Tsiambaos (2008))

Realistic consideration demands to incorporate also the strength of the rock matrix. This will lead to a curve like shown in Fig. 5b. For small and large angles β failure in the matrix is obtained, for other values of β failure along the plane of weakness is observed.

$$\sigma_1(\beta) = \sigma_3 + \frac{2\left[C_j + \sigma_3 \tan(\phi_j)\right]}{\left[1 - \tan(\phi_j)\tan(\beta)\right]\sin(2\beta)} \quad (1)$$

Anisotropy in strength is also observed under tensile loading. Fig. 6 shows different arrangements for Brazilian tests which cover all possible 3-dimensional constellations between loading direction and plane of anisotropy (plane of weakness). Usually, in 2-dimensional studies the strength anisotropy of rocks is tested against the angle β (foliation-loading angle) while the orientation angle ψ is assumed to be zero. However, as documented in Figures 7, 8, 9 and 10, the orientation angle plays also a significant role in characterizing the strength anisotropy. Rock strength anisotropy has been extensively investigated and many failure criteria have been deduced to predict the rock strength as a function of β (see also section 5.1).

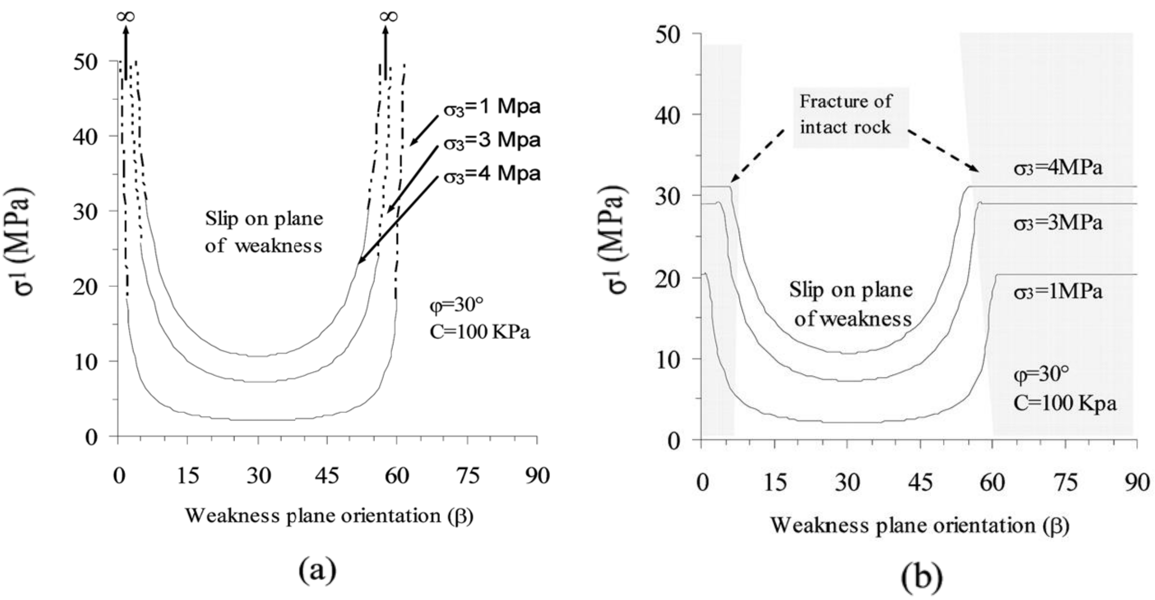

Fig. 5: Strength anisotropy: (a) theoretical solution according to Eq. 1, (b) realistic shoulder-shaped anisotropy (Bagheripour et al. 2011)

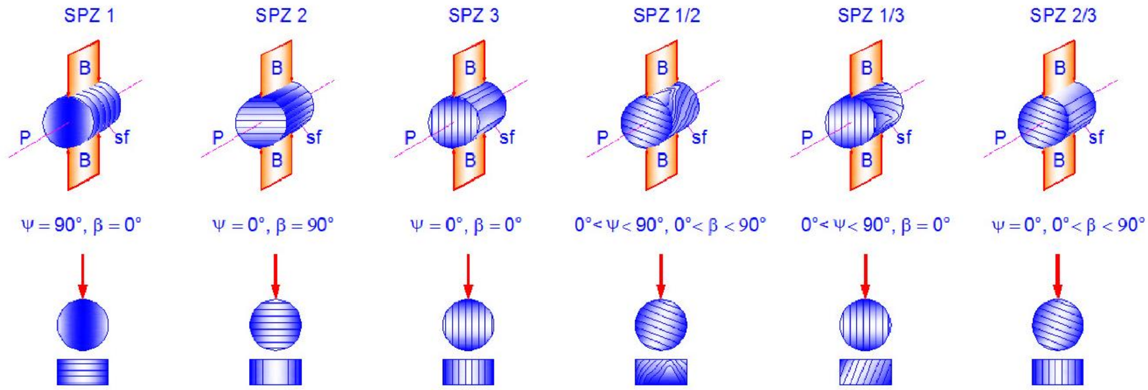

Fig. 6: Experimental arrangement for testing rock anisotropy relative to orientation angle ψ and foliation - loading angle β using the Brazilian test (Dinh et al. 2013).

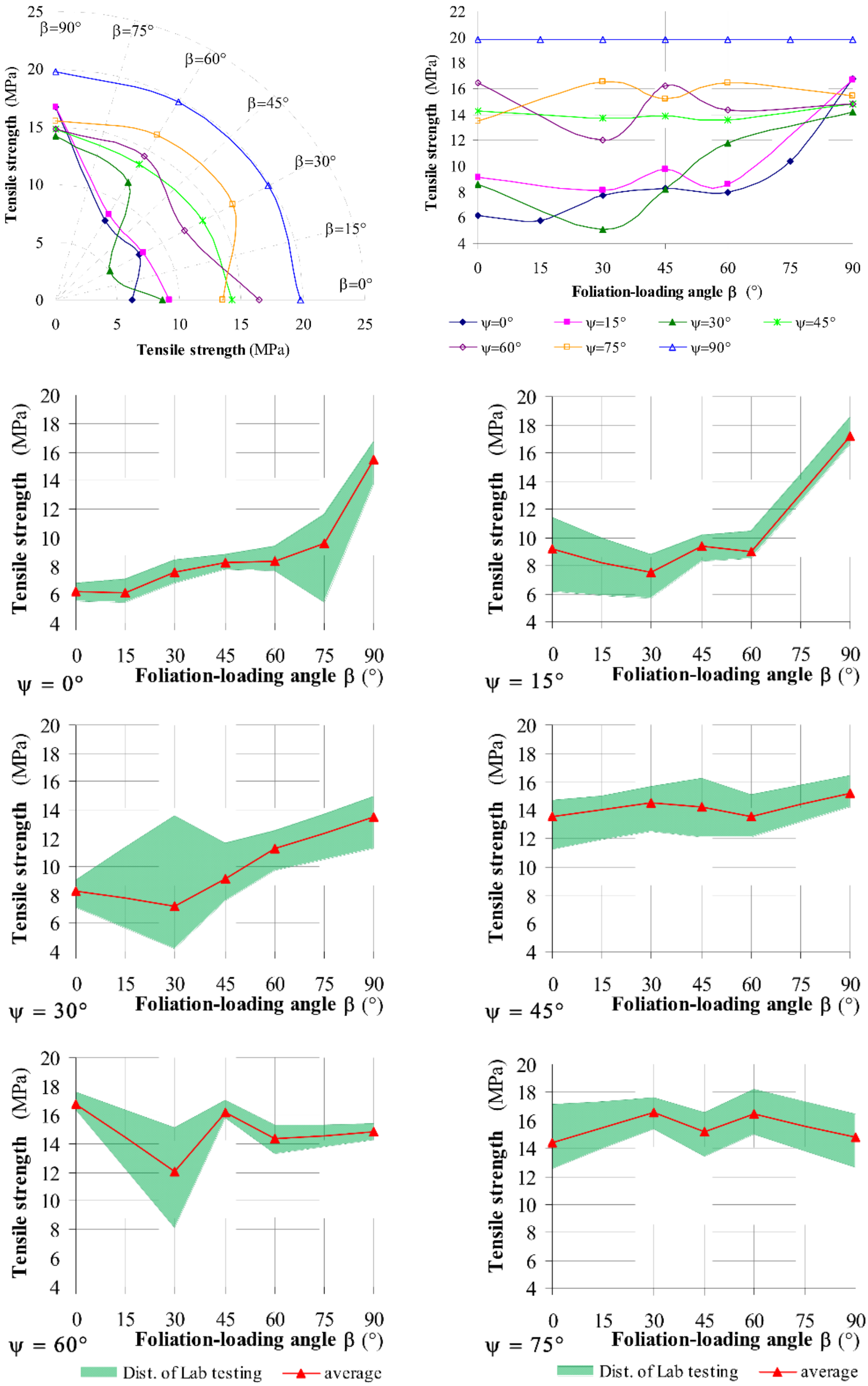

Fig. 7: Tensile strength results Gneiss samples as functions of β and ψ (Dinh et al. 2013)

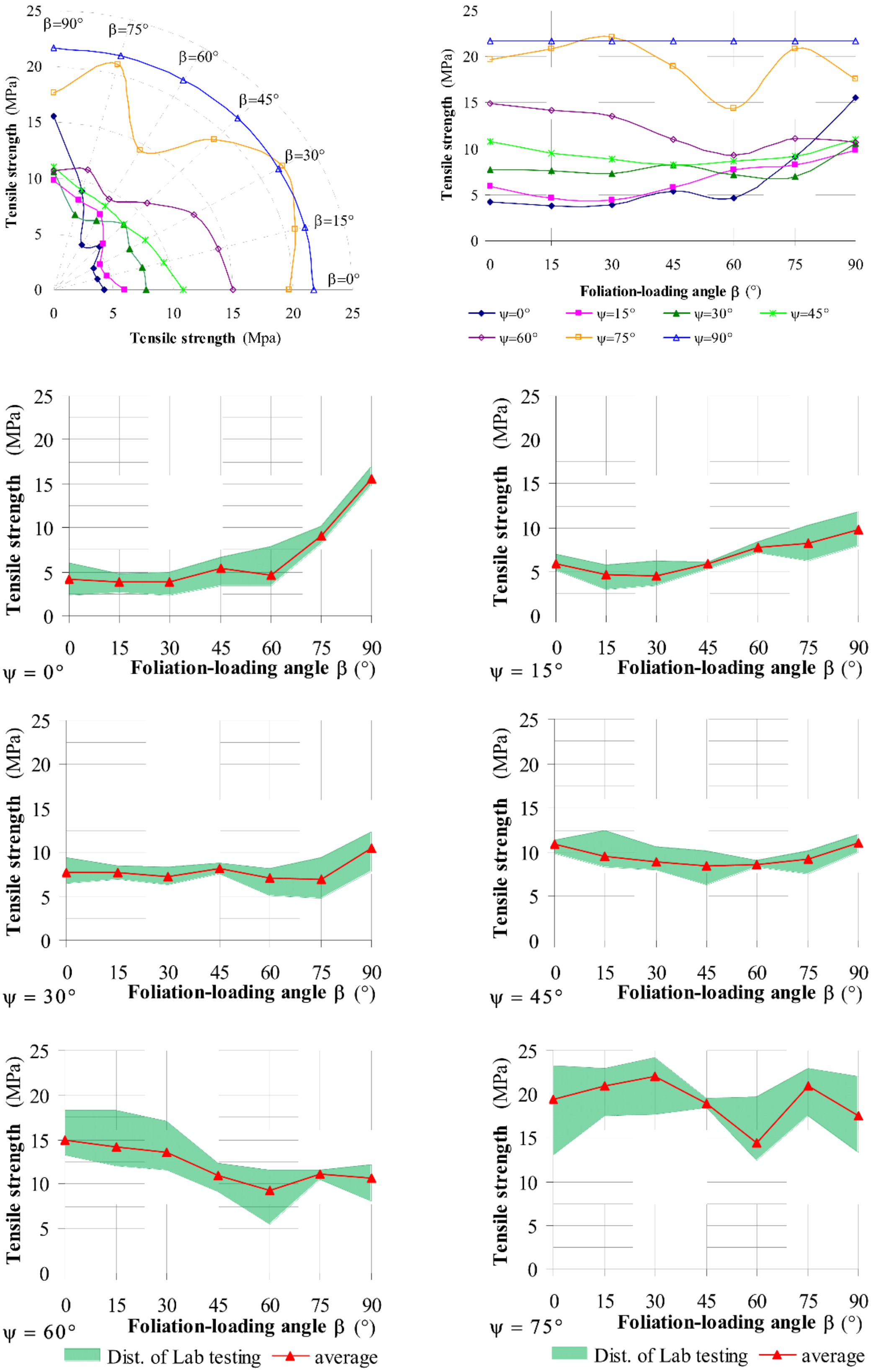

Fig. 8: Tensile strength results of Slate samples as functions of β and ψ (Dinh et al. 2013)

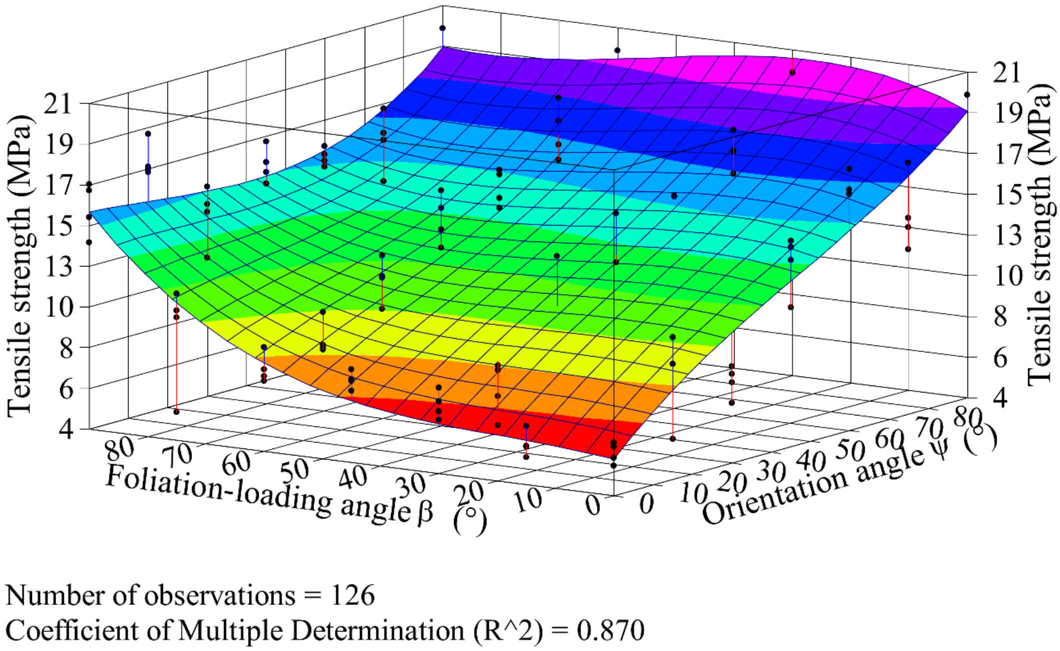

Fig. 9: Regression surface for tensile strength results of Gneiss samples as functions of β and ψ (Dinh et al. 2013)

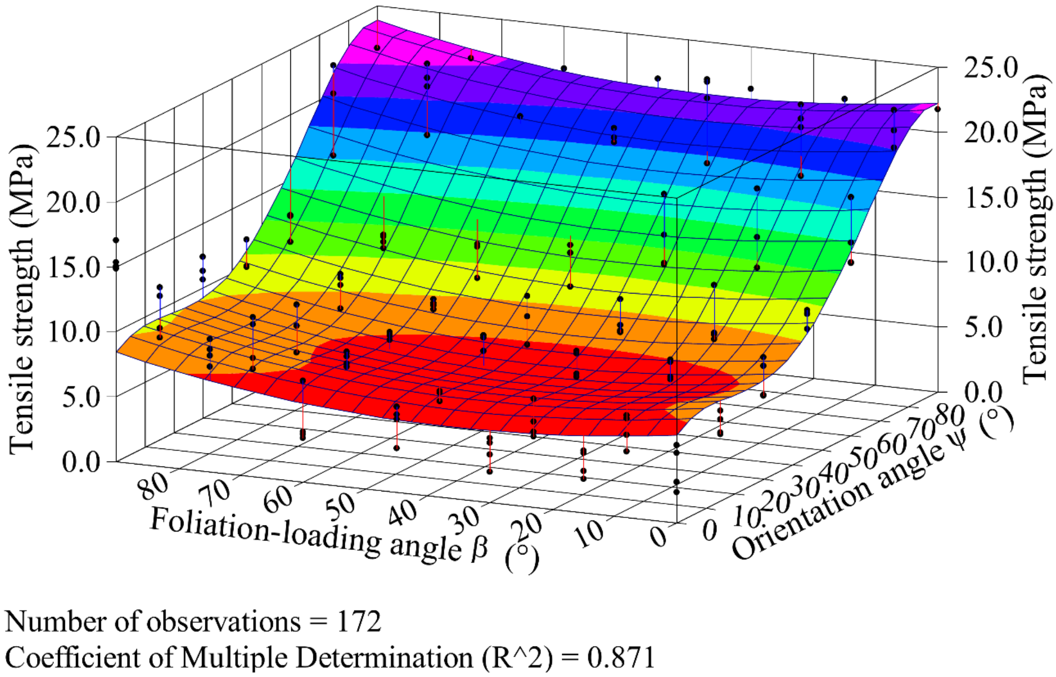

Fig. 10: Regression surface for tensile strength of Slate samples as functions of β and ψ (Dinh et al. 2013)

3.2 Stiffness anisotropy

Besides strength anisotropy, there exists also an anisotropy in stiffness, namely in terms of elastic constants like Young's modulus *E* or Poisson ratio ν.

Table 1: Elastic constants of Mayen-Koblenz Slate (Nguyen 2013)

Matrix Parameters	Unit	Min. – Max. Value	
		$\parallel$	$\perp$
Young's modulus	GPa	71 – 75	40 – 43
Poisson's ratio	-	0.25 – 0.3	0.23 – 0.3

$\parallel$ - Parallel to schistosity plane. $\perp$ - Perpendicular to schistosity plane

Table 1 shows the elastic properties of a slate measured parallel and perpendicular to the plane of anisotropy (schistosity plane). Stiffness parallel to the schistosity planes is much higher than those perpendicular to the schistosity planes. Park and Min (2015) have also tested gneiss and Schist. The YC schist shows stronger anisotropy in stiffness than the AS gneiss as documented in Fig. 11.

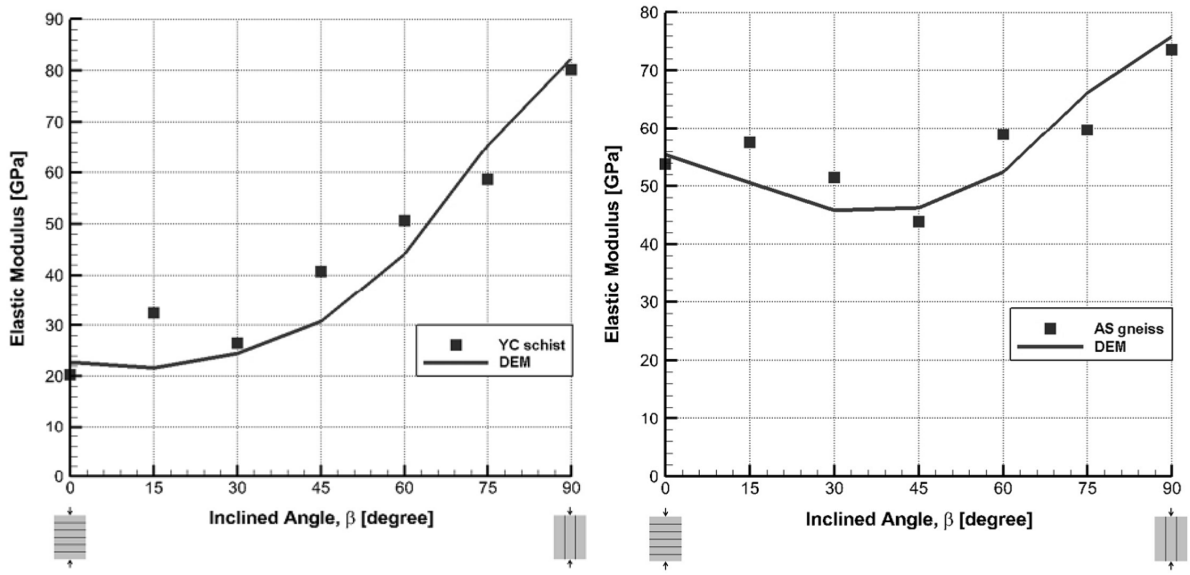

Fig. 11: Young's modulus for AS gneiss and YC Schist as function of angle β (Park and Min 2015)

3.3 Permeability anisotropy

Permeability anisotropy can be caused by bedding, schistosity, fractures, damage, stress level etc. Fig. 12 shows a typical example of a bedded sandstone with pronounced transverse isotropic permeability in the horizontal direction k_h and in the vertical direction k_v (Ayan et al. 1994). For anisotropy ratios >= 0.7 the material is considered to be quasi-isotropic (Meyer 2002). Another example is given by Mokhtari et al. (2013). They investigated permeability of six vertical, one inclined (45°) and one horizontal core samples of Mancos Shale. The permeability of this shale was studied in respect to the orientation of the bedding planes and the confining pressure as shown in Fig. 13. The samples are subjected to different confining pressures ranging from 1130 psi (≈7.79 MPa) to 3390 psi (≈ 23.37 MPa).

Fig. 12: Sandstone with pronounced permeability anisotropy, where $k_v / k_h \approx [0.1 \ldots 0.5]$ (Ayan et al. 1994)

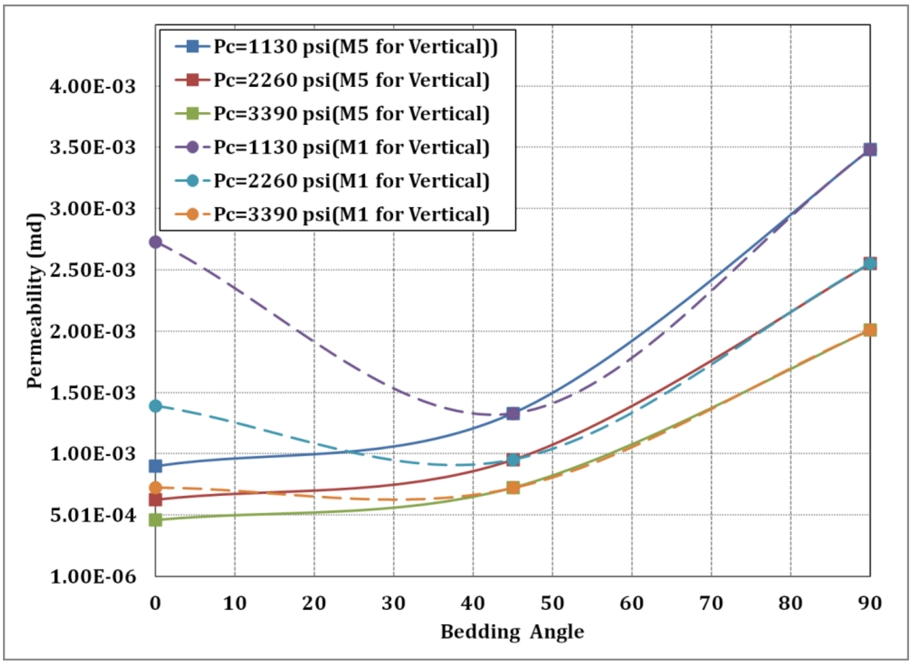

Fig. 13: Permeability anisotropy of Mancos Shale core samples (*Pc*: confining pressure; 1 psi = 0,0069 MPa) (Mokhtari et al. 2013)

3.4 Seismic anisotropy

Seismic anisotropy means that the wave propagation velocity depends on the propagation direction of the waves through the rock. Crampin (1981) has reviewed the theory of wave propagation for anisotropic elastic material. Fig (14) shows an example for transverse isotropic rocks. The wave speed is maximum (Vfast) in the direction parallel to the anisotropy plane and minimum (Vslow) perpendicular to this direction. It can be distinguished between P- and S-wave velocities (compressional and shear wave velocities). In addition, shear wave splitting or damping can be used to characterize anisotropy.

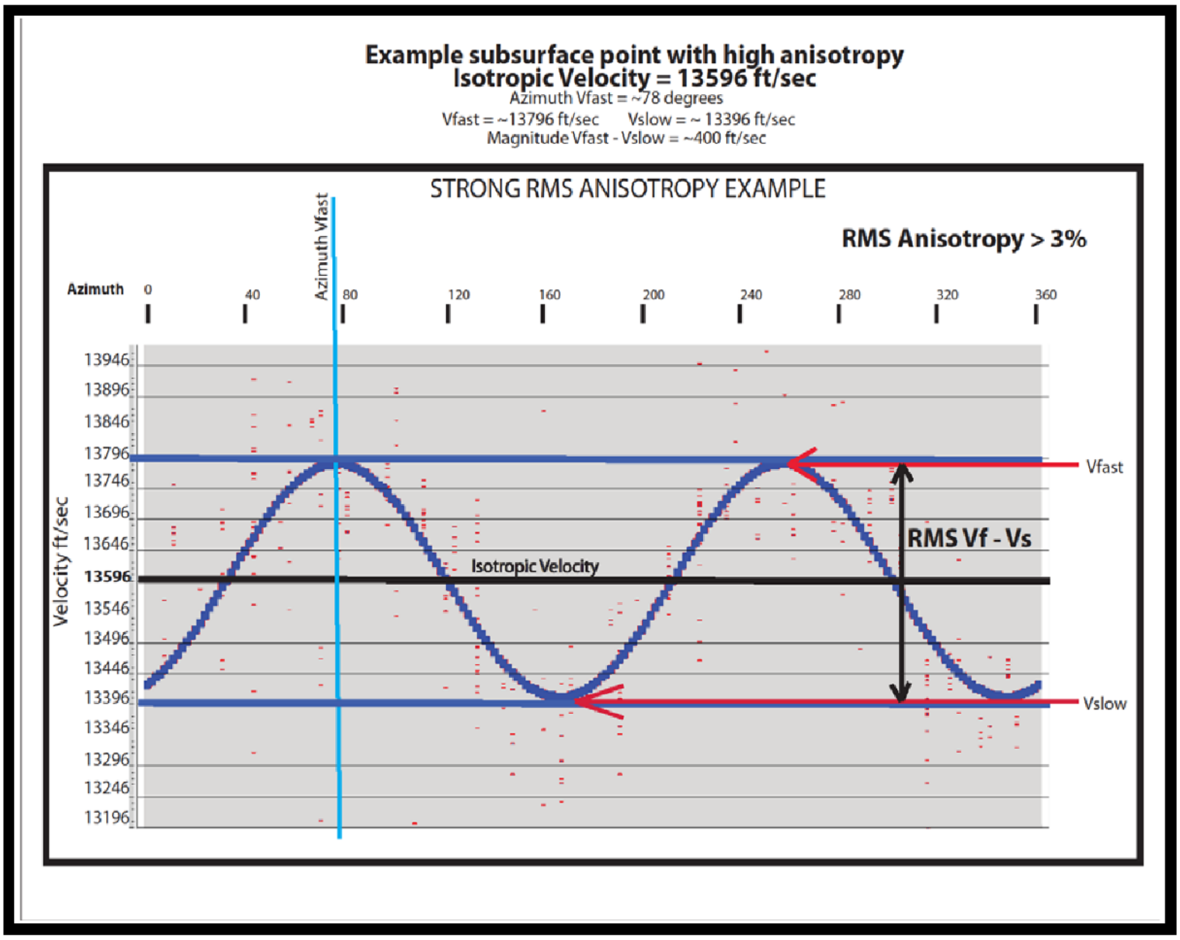

Fig. 14: Example of velocity anisotropy measured at cores (Root mean square of Vfast-Vslow > 3%, Inks et al. 2014)

4 Classification of rock anisotropy

Anisotropy of rocks can be quantified and classified (degree of anisotropy). There are several ways to classify rocks. Two often used systems are:

(i) The point load index
(ii) The strength anisotropy index.

4.1 Point load index

Tsidzi (1990) has proposed a classification for foliated rocks to classify the degree of foliation as well as the degree of anisotropy. A fabric index (Tsidzi, 1986) was introduced first to classify metamorphic rocks. Then, it has been noted that there is a strong relation between the degree of the foliation and the point load strength anisotropy index $I\alpha_{(50)}$ according to Eq. (2) which is proposed by the ISRM (1985).

$$I\alpha_{(50)} = \frac{I_{s(50)\perp}}{I_{s(50)\parallel}} \qquad (2)$$

$I_{s(50)\perp}$ and $I_{s(50)\parallel}$ are the point load strength indexes measured perpendicular and parallel to the foliation planes for a samples of diameter equal to 50 mm, perpendicular and parallel to the foliation planes at the axial and diametric test. According to the observations, the minimum point load value is found when the loading is parallel to the foliation planes and this is due to the splitting through these weakness planes (Saroglou & Tsiambaos 2007). Table 2 shows the proposed classification of foliated rocks based on the point load strength anisotropy index.

Table 2: Classification of foliated rocks based on strength anisotropy index (K. E. Tsidzi 1990)

Nature of rock	**Strength anisotropy Index $I\alpha_{(50)}$**	**Descriptive term**	**Examples**
Very strongly foliated	> 3.5	Very highly anisotropic	Slate
Strongly foliated	3.5 – 2.5	Highly anisotropic	Quartz mica schists
Moderately foliated	2.5 – 1.5	Moderately anisotropic	Mica gneisses
Weakly foliated	1.5 – 1.1	Fairly anisotropic	Granitic gneisses
Very weakly foliated or non-foliated	< 1.1	Quasi-isotropic	Quartzite

4.2 *Strength anisotropy classification (Rc)*

Ramamurthy (1993) defined the anisotropy strength (*Rc*), eq. (3) quantifies the *Rc* value as the ratio between strength of the intact rock of orientation angle ($\beta = 90°$) and the minimum strength of the same intact rock with orientation angle $\beta_0 = 0°$.

$$Rc = \frac{\sigma_{C(90)}}{\sigma_{C(\min)}} \tag{3}$$

This strength anisotropy classification based on *Rc*, shown in Table 3, evaluated for various rocks. Despite the fact that the degree of anisotropy defined by Rc is essentially based on uniaxial compressive strength of rock. However, reports on the strength anisotropy in confined compression state have shown that the degree of anisotropy for a specific rock is not constant (Zhang L. 2006).

As the effect of strength anisotropy is reduced when the confining pressure is increased, a newly introduced experimental criterion for discontinuous rock estimated a specific level of confining pressure about which the jointed weak sandstone ceased to behave as anisotropic rock (Bagheripour et al. 2011). This specific level of confining pressure σ_{3_0} was evaluated in terms of the uniaxial compressive strength of the corresponding intact rock as $\sigma_{3_0} = 0.58\sigma_{ci}$ which was also in well agreement with the relative value reported by (Ramamurthy & Arora 1994).

Table 3: Range of anisotropy strength and rock classes (Zhang L. 2006).

Anisotropic ratio *Rc*	**Class**	**Rock Types**
1.0 < Rc < 1.1	Isotropic	Sandstone
1.1 < Rc < 2.0	Low anisotropy	Sandstone, Shale
2.0 < Rc < 4.0	Medium anisotropy	Shale, Slate
4.0 < Rc < 6.0	High anisotropy	Slate, Phyllite
6.0 < Rc	Very high anisotropy	

5 Constitutive Modelling of rock anisotropy

A model is an approximation or abstract of the real states of the modelled media based on mathematical and physical equations. In such models assumptions are usually introduced. Rock strength anisotropy is the main concern of most of the constitutive models as well as the failure criterion which studies the rock behaviour under loading. A failure criterion can be defined according to Ambrose (2014) as follows:

> *"[A Failure criterion is] an equation that defines, either implicitly or explicitly, the value of the maximum principal stress that will be necessary in order to cause the rock to fail, which in the case of brittle behaviour can be interpreted as causing the rock to break along one or more failure planes."*

The failure of the rock happens when the stress state in the rock reaches its failure strength, which means either the stress state at which brittle rupture of the sample occurs, or the peak stress attained during large ductile deformation (Duveau, Shao, and Henry 1998).

Table 4: Classification of anisotropic failure criteria, (Duveau, Shao, and Henry 1998) and (Ambrose 2014)

Continuous Criteria		**Discontinuous Criteria**
Mathematical approach	**Empirical approach**	
Von Mises (1928)	Casagrande and Carrillo (1944)	Jaeger (1960, 1964)
Hill (1948)	Jaeger variable shear (1960)	Walsh and Brace (1964)
Olszak and Urbanowicz (1956)	McLamore and Gray (1967)	Hoek (1964, 1983)
Goldenblat (1962)	Ramamurthy, Rao and Singh (1988)	Murrell (1965)
Goldenblat and Kopnov (1966)	Ashour (1988)	Barron (1971)
Boehler and Sawczuk (1970, 1977)	Zhao, Liu and Qi (1992)	Ladanyi and Archambault (1972)
Tsai and Wu (1971)	Singh, et al. (1998)	Bieniawski (1974)
Pariseau (1968)	Tien & Kuo (2001)	Hoek and Brown (1980)
Boehler (1975)	Tien, Kuo and Juang (2006)	Smith and Cheatham (1980)
Dafalias (1979, 1987)	Tiwari and Rao (2007)	Yoshinaka & Yamabe (1981)
Allirot and Boehler (1979)	Saroglou and Tsiambaos (2007)	Duveau and Henry (1997)
Nova and Sacchi (1979)	Zhang & Zhu (2007)	Pei (2008)
Nova (1980, 1986)	Lee, Pietruszczak and Choi (2012)	Zhang (2009)
Boehler and Raclin (1982)		
Raclin (1984)		
Kaar et al. (1989)		
Cazacu (1995)		
Cazacu and Cristescu (1999)		

Kusabuka, Takeda and Kojo (1999)
Pietruszczak and Mroz (2001)
Lee and Pietruszczak (2007)
Mroz and Maciejewski (2011)

5.1 *Types of anisotropic rock failure criteria*

Various studies and analyses have been donated to investigate the rock anisotropy and specially the strength anisotropy. Out of these researches, many failure criteria have been introduced which tried to predict the behaviour of the anisotropic rocks under loading and therefore the rock strength. Duveau et al. (1998) have performed a classification of most of the introduced anisotropic rock failure criteria till 1998 and Ambrose (2014) has added the criteria which are developed till 2014, see Table 4. The classification of the failure criteria was mainly to both continuous and discontinuous criteria. For the continuous criteria, the rock material is considered as a continuous body with the assumptions of a continuous variation of strength. The continuous criteria are divided into both continuous criteria using mathematical approach and continuous criteria using empirical approach as shown in Table 5.

Table 5: Mathematical and empirical continuous criteria, based on Ambrose (2014), Duveau, Shao, and Henry (1998) and Dehkordi (2008).

Mathematical Continuous Criteria	**Empirical Continuous Criteria**
Definition: A criterion at which the strength function is generally described by a mathematical technique, which considers the type of symmetries existing in the material. Out of these criteria, number of constants are generated.	***Definition:*** They are an extension from isotropic failure criterion to describe the anisotropic strength by empirical laws that define the variation of material parameters with respect to loading orientation. The various parameters are determined from fitting experimental data.
Representative Criterion: One of the main and first criteria is Hill's principal for frictionless materials which is an extension of the Von-Mises isotropic theory. (Pariseau 1968) extended Hill's criterion for cohesive-frictional material like rocks.	***Representative Criterion:*** Jaeger (1960) had proposed a criterion called "the variational cohesion theory" at which Mohr-Coulomb had been altered using variable material cohesion as a function of loading orientation and a constant value of friction.
Challenges: 1) The determination of material constants which should be determined experimentally, and 2) Each criterion has its own opinion on the anisotropy depending on the insight into the physical behaviour of the material or the tested rocks.	***Challenges:*** 1) The determination of such criterion requires a large amount of experimental data, as well as an appropriate curve-fitting process, and 2) There is lack in the physical and mathematical basis of such criteria.

On the contrary, the discontinuous criteria at which *“the basic assumption is that the failure of an anisotropic body is due to either the fracture of bedding planes or the fracture of the rock matrix and two distinct criteria should be used for the two fracture modes”* (Duveau et al., 1998). Fig. 5 illustrates the idea of discontinues criteria and how different distinct criteria can be used to describe the failure mechanisms activated in the material elastic response of anisotropic rock.

5.2 Elastic response of anisotropic rock

The behaviours of the rocks depend basically on both theories of elasticity and plasticity. In such context brittle rocks use the basics of elasticity theory to analyse the stress strain behaviour. Generally, the rock materials can be defined as elastic when at loading – unloading cycle they reach their first state with no changes. This is called reversible nature (Elmo 2006). Hooke’s law illustrates the linear behaviour of the elastic material. Eq. (4) states that stress (σ_{ij}) is linearly proportional to strain (ε_{ij}) (Mavko et al., 1998). This relation is altered to quantify the anisotropic nature of rocks.

$$\sigma_{ij} = C_{ijkl} \chi \varepsilon_{kl} \tag{4}$$

Where, σ_{ij} is the stress state, ε_{kl} is the strain state in 2-D medium, and C_{ijkl} is the fourth-rank elastic stiffness tensor. In its most general form – in three-dimensional (3D) space – the elasticity matrix has 81 components. The fourth rank elastic stiffness tensor is reduced to maximum 21 independent components, due to the symmetry concept in this tensor between both the stress and the strain and also the existence of a unique strain-energy potential based on the conservative law of energy (Zang and Stephansson 2010).

Before we discuss the elastic symmetry and the different independent components of the elastic tensor, we have to know the difference between tensor and matrix. In Voigt notation (Voigt 1966), the symmetric second-order stress and strain tensors reduce to 6-component vectors and the fourth-rank elastic tensor reduces to a six by six second-rank matrix (Dehkordi 2008). Generally, the fourth-rank tensor C_{ijkl} with the 81 components is replaced because of the symmetry with the expression the elastic tensor C_{ab}.

5.2.1 Orthotropy

For orthogonal anisotropic (orthotropic) rocks, e.g.: a rock mass with three sets of orthogonal fractures (three planes of elastic symmetry) having different properties. It is assumed that (i) these planes exist at each point in the rock, and (ii) these planes have the same orientation throughout the rock (Amadei 1996). The deformability of rocks such as coal, schists, granites and sandstone shows the orthogonal anisotropic nature, see Fig. 15. In this type of anisotropy, the rock material has more than one plane of symmetry up to three orthogonal planes of symmetry, as it is illustrated in Fig. 15. The model is called the orthotropic model which involves nine independent elastic constants:

E_1, E_2, E_3 Young’s moduli in the directions of *local* axes.

G_{12}, G_{23}, G_{13} Shear moduli in planes parallel to the *local* coordinate planes.

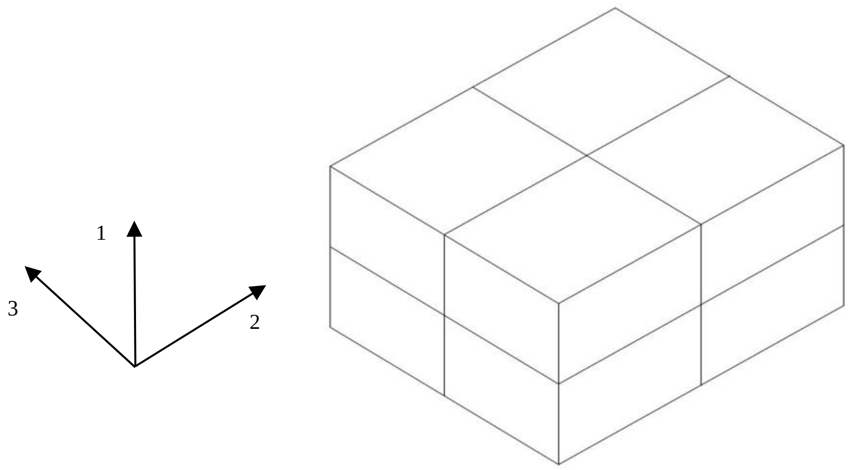

Fig. 15: Schematic of orthotropic rock

ν_{12}, ν_{23}, ν_{13} Poisson's ratio where ν_{ij} characterizes lateral contraction in *local* direction i caused by loading in *local* direction j.

The stiffness matrix C_{ab} definition of the orthotropic anisotropic rocks is very complicated, that is why we define the nine independent elastic constants using the compliance matrix (D_{ab}), as in eq. (5); where, $C_{ab} = D_{ab}^{-1}$ and $D_{ab} = C_{ab}^{-1}$.

$$D_{a,b} = \begin{bmatrix} \frac{1}{E_1} & -\frac{\nu_{12}}{E_2} & -\frac{\nu_{13}}{E_3} & 0 & 0 & 0 \\ -\frac{\nu_{12}}{E_1} & \frac{1}{E_2} & -\frac{\nu_{23}}{E_3} & 0 & 0 & 0 \\ -\frac{\nu_{13}}{E_1} & -\frac{\nu_{23}}{E_2} & \frac{1}{E_3} & 0 & 0 & 0 \\ 0 & 0 & 0 & \frac{1}{2G_{23}} & 0 & 0 \\ 0 & 0 & 0 & 0 & \frac{1}{2G_{13}} & 0 \\ 0 & 0 & 0 & 0 & 0 & \frac{1}{2G_{12}} \end{bmatrix} \quad (5)$$

5.2.2 Transverse isotropy

Transverse isotropy is often used to describe the symmetry of rocks with one dominant system of layers (e.g., bedding, layering, and foliation), see Fig. 16. In this case, five elastic constants are used in a reference frame attached to the rock layers. The transversely isotropic nature appears at the macro scale due to the planes of weaknesses which is found in most of metamorphic rocks such as: slates, gneisses, phyllites and schists. In the forming process rocks flow and recrystallize under new tectonic stresses and form such weak foliation planes (Saeidi et al. 2013).

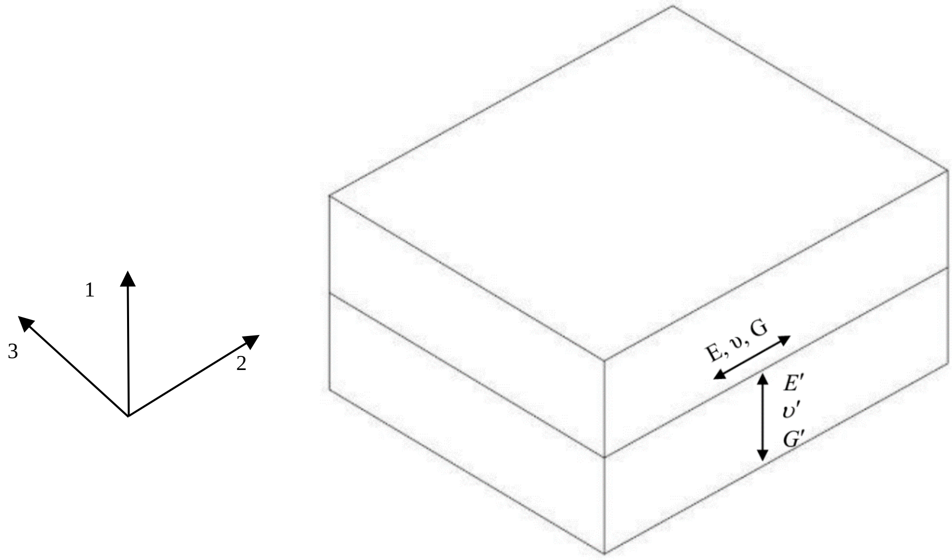

Fig. 16: Schematic of the transverse isotropy and this model parameters

The model involves the five independent elastic constants E, E', ν, ν' and G'. The five independent elastic constants of the stiffness matrix as in eq. 6 are described as:

(1) E and E´ are Young's moduli in the plane of the weakness plane (transverse isotropy plane) and in normal direction to this plane,

(2) ν and ν' are Poisson ratios in the same directions of Young's moduli, and

(3) G´ is the shear modulus normal to the plane of weakness (Amadei, 1996).

These planes of weakness (i.e. schistosity and foliation) are assumed to be parallel to the plane of the transverse isotropy which affect the behaviour of the stiffness matrix. The local stiffness matrix is indicated in eq.6 (Jing, L. & Stephenson 2007).

$$C_{ab} = \begin{bmatrix} C_{11} & C_{12} & C_{13} & 0 & 0 & 0 \\ C_{12} & C_{11} & C_{13} & 0 & 0 & 0 \\ C_{13} & C_{13} & C_{33} & 0 & 0 & 0 \\ 0 & 0 & 0 & C_{44} & 0 & 0 \\ 0 & 0 & 0 & 0 & C_{44} & 0 \\ 0 & 0 & 0 & 0 & 0 & (C_{11}-C_{12})/2 \end{bmatrix} \quad (6)$$

Where, $C_{11} = C\left(\frac{1}{EE'} - \frac{\nu'^2}{E'^2}\right)$, $C_{12} = C\left(\frac{\nu}{EE'} - \frac{\nu'^2}{E'^2}\right)$, $C_{13} = C\frac{(1+\nu)\nu'}{EE'}$, $C_{33} = C\frac{1-\nu^2}{E^2}$, $C_{44} = G'$ and $C = \frac{E^2E'^2}{(1+\nu)\left[(1-\nu)E' - 2\nu'^2 E\right]}$

The shear modulus, G, is not independent and it can be calculated by eq. (7):

$$G = \frac{E}{2(1+\nu)} \tag{7}$$

Besides the five properties, the orientation of the isotropic plane also need to be given its direction. Lekhnitskii (1981) using the following equation to determine the cross shear modulus for anisotropic elasticity, G', which bases on lab testing of rock (Hwu 2010).

$$G_{12}(G') = \frac{EE'}{E(1+2\upsilon')+E'} \tag{8}$$

5.2.3 Elastic isotropy

For isotropic elastic rocks, the elasticity matrix is supposed to be symmetric in all directions. Through the derivation of the elastic tensor, the system can described by only two elastic constants which represent two independent elastic coefficients. The two elastic constants are Poisson's ratio (ν) and Young's modulus (E), the elasticity matrix can be written as in eq. (9) (Jing, L. & Stephenson 2007).

$$C_{ab} = \begin{bmatrix} C_{11} & C_{12} & C_{12} & 0 & 0 & 0 \\ C_{12} & C_{11} & C_{12} & 0 & 0 & 0 \\ C_{12} & C_{12} & C_{11} & 0 & 0 & 0 \\ 0 & 0 & 0 & (C_{11}-C_{12})/2 & 0 & 0 \\ 0 & 0 & 0 & 0 & (C_{11}-C_{12})/2 & 0 \\ 0 & 0 & 0 & 0 & 0 & (C_{11}-C_{12})/2 \end{bmatrix} \tag{9}$$

Where $C_{11} = \frac{E}{1+\nu}\frac{1-\nu}{1+\nu}$ and $C_{12} = \frac{E}{1+\nu}\frac{\nu}{1+2\nu}$.

Finally, Rock material is considered in the elastic behaviour either isotropic elastic when we are dealing with brittle rocks or with the intact flawless rock which is a very rare condition. Otherwise, we can consider it as anisotropic elastic which means the anisotropic rocks are transverse isotropic or orthotropic.

5.3 Plastic response of anisotropic rock

The stress-strain behaviour has a nonreversible part which refers to the plastic nature of the rock material. This stage of nature always positioning directly after the elastic part on the stress-strain curve which describes the behaviour of the rocks under loading.

5.3.1 Introduction

It is essential to describe the elastoplastic behaviour in multiaxial stress conditions to define the following:
Yield surface (F) is the stress state at which the yielding deformation may progress or in other words a failure criterion. The yield conditions for an interface in which β are the orientation of applied load with respect to state of stress, σ and the hardening parameter, k_h, as in eq. (10).

$$F(\sigma, k_h, \beta) = 0 \tag{10}$$

The most usable failure criterion for rocks is the Mohr-Coulomb-Criterion which is written in principle stresses as in eq. (11).

$$f = \sigma_1 - \sigma_3 - (\sigma_1 + \sigma_3)\sin\varphi - 2c\cos\varphi = 0 \tag{11}$$

M-C failure criterion has been upgraded for rocks, as it is seen in Fig. 17, by adding a tension-cut off part into the original criterion, (Vermeer 1998).

The Plastic potential *Q* as given in eq. (12) determines the direction of plastic straining after yield is reached (Dehkordi, 2008).

$$Q(\sigma) = \text{const.} \tag{12}$$

The association between both functions the yield function and plastic potential function $F(\sigma, k_h) = Q(\sigma)$ is called associated flow rule, but when $F(\sigma, k_h) \neq Q(\sigma)$ it is non-associated flow condition, (Vermeer, Pieter A & De Borst 1984).

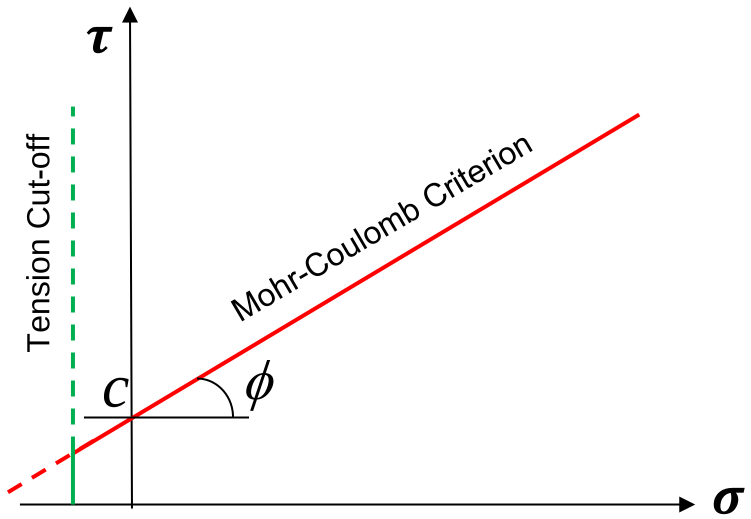

Fig. 17: Mohr-Coulomb failure criterion with a tension cut-off

5.3.2 Continuum vs. discontinuum approach

For anisotropic rocks, the plastic behaviour can be modelled using the same procedure as in part (5.3.1). However, there are two major approaches that can be used for the same procedure: The continuum and discontinuum approaches. Table 6 shows the main differences between both approaches.

Table 6 Comparison between continuum and discontinuum approaches

Continuum approach	**Discontinuum approach**
Benefits and usability: 1) The numerical discretization is independent of the joints reduces the model size and increases computational efficiency. 2) Computation time is much lower than discontinuous modelling.	*Benefits and usability:* 1) Simulate both micro- or macro-scale discontinues. 2) It allows finite displacements and rotations of discrete bodies, including complete detachment and generate new contacts automatically.
Drawbacks: 1) Geometry of discontinuities is restricted. 2) For every time-step especially when significant displacement is noticed along the discontinuity, remeshing is required for the entire model which leads to numerical instabilities.	*Drawbacks:* 1) Duration of a virtual simulation is limited by computational power. 2) The reliability of the results is highly dependent on the input parameters which are difficult to confirm.
Most popular methods: - Finite Element Method (FEM) - Boundary Element Method (BEM) - Finite Difference Method (FDM)	*Most popular methods:* - Distinct Element Method (DEM) - Discontinuous Deformation Analysis (DDA) - Finite Element Method with interface model (FEM*).

5.3.3 Single surface plasticity

It is called single surface plasticity when it requires only one failure criterion (yield surface) and one plastic potential function therefore to describe the plastic behaviour of the anisotropic rock. As it is introduced in 5.3.1 and in 5.3.2, we are going to deriving two examples which discuss the single surface plasticity based on the Ubiquitous Joint model.

In the first case, a static uniaxial compressive loading is applied on a rock sample having one joint plane, while in the second case, the rock sample has two orthogonal joint planes, as in Fig. 18. The two rock samples have the same dimensions and properties. The uniaxial compressive strength of a jointed rock sample is a function of the angle formed by the major principal stress and the joints, Table 7.

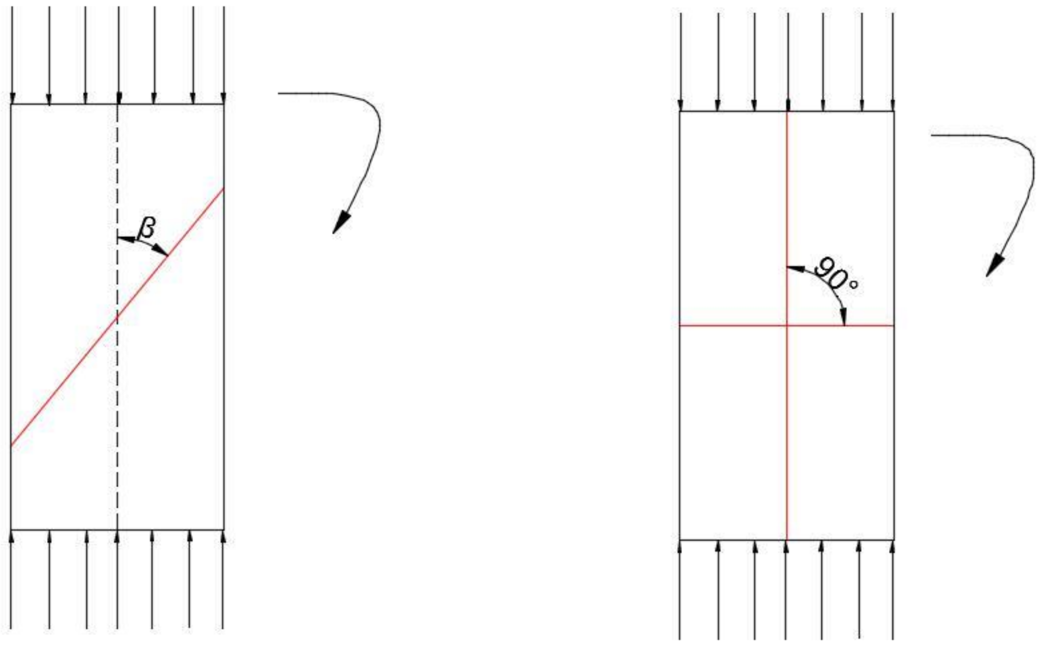

Fig. 18: The two tested samples simulated with FLAC 7.0

Table 7: Two examples for jointed rocks using single plane of plasticity approach of the ubiquitous-joint model.

Sample with one Joint plane	**Sample with two perpendicular joint planes**
Analytical basics:	
The plane-of-weakness model (Jaeger, J. C. & Cook 1979): $$\sigma_1 = \frac{2c_j}{1-\tan\varphi_j \tan\beta}\sin(2\beta)$$	
Comparison with analytical solution:	
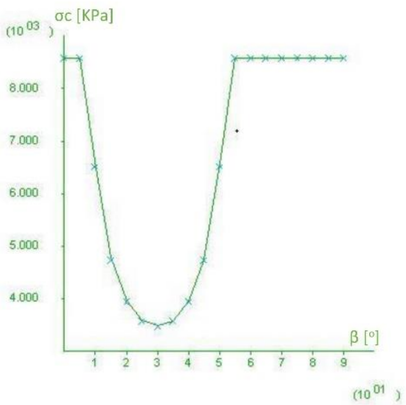	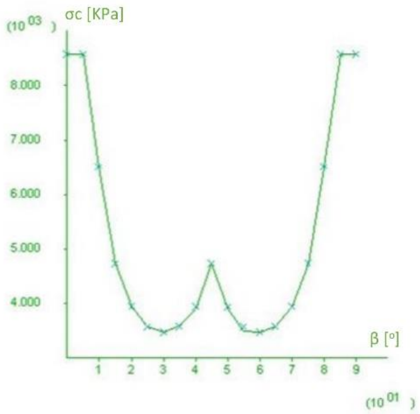
strength of ubiquitous-joint model (cross) versus analytical solution (line)	

5.3.4 Remarks on anisotropic rock constitutive modelling

A. Rock strength of jointed rock depends completely on the degree of the interlocking of rock blocks. Rocks with a single joint set behave highly anisotropic, while the strength behaviour of rock masses having three, four or five intersecting joint sets are considered approximately as homogenous and isotropic rocks (Hoek 1983).

B. The elastic stiffness matrix C_{ab} for rock material could be transverse isotropic or orthotropic, but it cannot be neither monoclinic symmetric (one plane of symmetry, 13 independent elastic coefficients) nor triclinic symmetry (known also as allotropic; no planes of symmetry, 21 independent elastic coefficients).

C. In more complicated cases it is almost impossible to get all the parameters of Hook's law to study rock mass behaviour.

D. Usually a non-associated flow rule is considered in the plastic framework of the anisotropic rocks in which $F(\sigma, k_h) \neq Q(\sigma)$.

E. The failure of the anisotropic rocks usually depends on the discontinuous planes of weakness models in which the failure of an anisotropic body is either the result of failure of one or more weakness planes or the result of failure of the intact matrix.

F. Based on (E) , multiple failure criterion are adopted to describe the failure mechanism which leads, in the plastic behaviour, to the multi-surface plasticity which is applied to rock mechanics problems where a matrix of intact material is intersected with one or multiple sets of joints.

6 Literature

Amadei, B. 1996. “Importance of Anisotropy When Estimating and Measuring in Situ Stresses in Rock.” *International Journal of Rock Mechanics and Mining Sciences & Geomechanics Abstracts* 33(3): 293–325. http://linkinghub.elsevier.com/retrieve/pii/0148906295000623.

Ambrose, Jasmin. 2014. *Failure of Anisotropic Shales under Triaxial Stress Conditions, PhD Thesis*. Imperial College London: Department of Earth Science and Engineering.

Ayan, C. et al. 1994. “Measuring Permeability Anisotropy: The Latest Approach.” *Oilfield Review* 6(4): 24–35. http://199.6.139.141/media/services/resources/oilfieldreview/ors94/1094/p24_35.pdf.

Bagheripour, Mohammad Hossein, Reza Rahgozar, Hassan Pashnesaz, and Mohsen Malekinejad. 2011. “A Complement to Hoek-Brown Failure Criterion for Strength Prediction in Anisotropic Rock.” *Geomechanics and Engineering* 3(1): 61–81.

Bobet, A. et al. 2009. “Numerical Models in Discontinuous Media: Review of Advances for Rock Mechanics Applications.” *Journal of Geotechnical and Geoenvironmental Engineering* 135(11): 1547–61. http://ascelibrary.org/doi/10.1061/%28ASCE%29GT.1943-5606.0000133.

Crampin, Stuart. 1981. “A Review of Wave Motion in Anisotropic and Cracked Elastic-Media.” *Wave Motion* 3(4): 343–91.

Dehkordi, Azadeh. 2008. *3D Finite Element Cosserat Continuum Simulation of Layered Geomaterials, PhD Thesis*. University of Toronto: Department of Civil Engineering.

Dinh, Q., Konietzky, H. & Herbst, M. 2013. "Brazilian tensile strength tests on some anisotropic rocks", Int. J. Rock Mech. Rock Sciences, 58: 1-7

Donath, F. A. 1966. “A Triaxial Pressure Apparatus for Testing of Consolidated or Unconsolidated Materials Subject to Pore Pressure.” *In Testing Techniques for Rock Mechanics (ASTM Spec. Tech.)* Pub. 402: 41–51.

Duveau, G., J. F. Shao, and J. P. Henry. 1998. “Assessment of Some Failure Criteria for Strongly Anisotropic Geomaterials.” *Mechanics of Cohesive-Frictional Materials* 3(1): 1–26.

Elmo, Davide. 2006. “Evaluation of a Hybrid FEM/DEM Approach for Determination of Rock Mass Strength Using a Combination of Discontinuity Mapping and Fracture Mechanics Modelling, with Particular Emphasis on Modelling of Jointed Pillars.” (March).

Van Hise, R. C. 1896. “Deformation of Rocks.: III. Cleavage and Fissility.” *The Journal of Geology* 4(4): 449–83. http://www.jstor.org/stable/30054934.

Hoek, Evert. 1983. “Strength of Jointed Rock Masses.” *Geotechnique* 23(3): 187–223.

Hudson, J.A. & Harrison, J.P. 1997. “Preface.” In *Engineering Rock Mechanics*, Elsevier, 163–64. http://linkinghub.elsevier.com/retrieve/pii/B978008043864150001X.

Hwu, Chyanbin. 2010. “Anisotropic Elastic Plates.” : 29–53. http://link.springer.com/10.1007/978-1-4419-5915-7.

Inks, Tanya L et al. 2014. “Comparison of Marcellus Fracturing Using Azimuthal Seismic Attributes Versus Published Data From Outcrop Studies.” *Proceedings of the 2nd Unconventional Resources Technology Conference* (1): 1–19. http://search.datapages.com/data/doi/10.15530/urtec-2014-1922505.

ISRM. 1985. “Suggested Method for Determining Point Load Strength.” *Int. J. Rock Mech. Min. Sci. & Geomech. Abstr.* 22: 51–60. http://www.geoplanning.it/test/wp-content/uploads/2012/02/Suggest-method-for-determining-Point-Load-Strength.pdf.

Itasca Consulting Group. 2007. *FLAC. Fast Lagrangian Analysis of Continua: Constitutive Models*. Minneapolis MN, USA.

Jaeger, J. C. 1960. “Shear Failure of Anisotropic Rocks.” *Geological Magazine* 97(1): 65–72. http://geolmag.geoscienceworld.org/content/97/1/65.abstract (March 7, 2016).

Jaeger, J. C. & Cook, N. G. 1979. *Fundamental of Rock Mechanics*. 3rd ed. London: Chapman and Hall.

Jing, L. & Stephenson, O. 2007. *Fundamentals of Discrete Element Methods for Rock Engineering: Theory and Applications*. 1st ed. Elsevier Science.

Matsukura, Y., K. Hashizume, and C. T. Oguchi. 2002. “Effect of Microstructure and Weathering on the Strength Anisotropy of Porous Rhyolite.” *Engineering Geology* 63(1-2): 39–47.

Mavko, G., Mukerji, T. & Dvorkin, J. 1998. *The Rock Physics Handbook: Tools for Seismic Analysis in Porous Media*. Cambridge: Cambridge University Press.

Meyer, Rudi. 2002. “Anisotropy of Sandstone Permeability.” *CREWES Reaserch Report* 14: 1–12. http://crewes.org/ForOurSponsors/ResearchReports/2002/2002-05.pdf.

Mokhtari, Mehdi, Adel a. Alqahtani, Azra N. Tutuncu, and Xiaolong Yin. 2013. “Stress-Dependent Permeability Anisotropy and Wettability of Shale Resources.” In *Unconventional Resources Technology Conference, Denver, Colorado, 12-14 August 2013*, Denver, Colorado: Society of Exploration Geophysicists, American Association of Petroleum Geologists, Society of Petroleum Engineers, 2713–28. http://library.seg.org/doi/abs/10.1190/urtec2013-283.

Nguyen, Van Manh. 2013. *Static and Dynamic Behaviour of Joints in Schistose Rock : Lab Testing and Numerical Simulation, PhD Thesis*. TU Bergakademie Freiberg: Institut fuer Geotechnik. http://tubaf.qucosa.de/fileadmin/data/qucosa/documents/12629/Thesis_VanMan h Nguyen 2013.pdf.

Pariseau, William G. 1968. “Plasticity Theory For Anisotropic Rocks And Soil.” In *The 10th U.S. Symposium on Rock Mechanics (USRMS)*, Austin, Texas: American Rock Mechanics Association.

Park, Bona, and Ki-Bok Min. 2015. “Bonded-Particle Discrete Element Modeling of Mechanical Behavior of Transversely Isotropic Rock.” *International Journal of Rock Mechanics and Mining Sciences* 76: 243–55. http://linkinghub.elsevier.com/retrieve/pii/S1365160915000647.

Priest, Stephen D. 1993. *Discontinuity Analysis for Rock Engineering*. Dordrecht: Springer Netherlands. http://link.springer.com/10.1007/978-94-011-1498-1.

Ramamurthy, T. 1993. “Strength and Modulus Responses of Anisotropic Rocks.” *Comprehensive rock engineering* 1: 313–29.

Ramamurthy, T., and V. K. Arora. 1994. “Strength Predictions for Jointed Rocks in Confined and Unconfined States.” *International Journal of Rock Mechanics and Mining Sciences and* 31(1): 9–22.

Saeidi, Omid, Rashid Geranmayeh Vaneghi, Vamegh Rasouli, and Raoof Gholami. 2013. “A Modified Empirical Criterion for Strength of Transversely Anisotropic Rocks with Metamorphic Origin.” *Bulletin of Engineering Geology and the Environment* 72(2): 257–69.

Salager, Simon, Bertrand François, Mathieu Nuth, and Lyesse Laloui. 2013. “Constitutive Analysis of the Mechanical Anisotropy of Opalinus Clay.” *Acta Geotechnica* 8(2): 137–54.

Saroglou, H, and G Tsiambaos. 2007. “Classification of Anisotropic Rocks.” In *11th Congress of the International Society for Rock Mechanics*, ed. Ribeiro e Sousa. Taylor & Francis Group, 191–96.

Saroglou, H., and G. Tsiambaos. 2008. “A Modified Hoek-Brown Failure Criterion for Anisotropic Intact Rock.” *International Journal of Rock Mechanics and Mining Sciences* 45(2): 223–34.

Singhal, B. B S, and R. P. Gupta. 2010. “Applied Hydrogeology of Fractured Rocks: Second Edition.” *Applied Hydrogeology of Fractured Rocks: Second Edition*: 1–408.

Thomsen, Leon. 1986. “Weak Elastic Anisotropy.” *Geophysics* 51(10): 1954–66.

Tsidzi, K. E. N. 1986. “A Quantitative Petrofabric Characterization.” *Bull. Int. Assoc. Eng. Geol.* 33: 3–12.

Tsidzi, Kwami Edwin. 1990. “The Influence of Foliation on Point Load Strength Anisotropy of Foliated Rocks.” *Engineering Geology* 29(1): 49–58.

Tsvankin, Ilya et al. 2010. “Seismic Anisotropy in Exploration and Reservoir Characterization: An Overview.” *Geophysics* 75(5): 75A15.

Ullemeyer, Klaus, Siegfried Siegesmund, Patrick N J Rasolofosaon, and Jan H. Behrmann. 2006. “Experimental and Texture-Derived P-Wave Anisotropy of Principal Rocks from the TRANSALP Traverse: An Aid for the Interpretation of Seismic Field Data.” *Tectonophysics* 414(1-4): 97–116.

Vermeer, P A. 1998. “Non-Associated Plasticity for Soils, Concrete and Rock.” In *Physics of Dry Granular Media*, Dordrecht: Springer Netherlands, 163–96. http://link.springer.com/10.1007/978-94-017-2653-5_10.

Vermeer, Pieter A & De Borst, R. 1984. “Non-Associated Plasticity for Soils, Concrete and Rock.” *HERON* 29(3): 3–64.

Voigt, Woldemar. 1966. *Lehrbuch Der Kristallphysik*. Wiesbaden: Vieweg+Teubner Verlag. http://link.springer.com/10.1007/978-3-663-15884-4.

Walhlstrom, E. E. 1973. *Tunnelling in Rock*. 1st ed. Amsterdam: Elsevier.

Zang, Arno, and Ove Stephansson. 2010. *Stress Field of the Earth’s Crust*. Dordrecht: Springer Netherlands. http://link.springer.com/10.1007/978-1-4020-8444-7.

Zhang L. 2006. “Engineering Properties of Rocks.” ed. John Hudson. *Elsevier Geo-Engineering Book Series* 4: 226–30.